

RESEARCH ARTICLE

Metal Complexes of Ligand Derived from Amine Compound: Formation, Spectral Characterization, and Biological Evaluation

Wisam A. Abdulrahman,¹ Iman A. Othman,¹ Enass J. Waheed²

¹Department of Chemistry, College of Education for Faculty, University of Samarra, Samarra, Iraq

²Department of Chemistry, College of Education for Pure Sciences, Ibn-Al-Haitham, University of Baghdad, Baghdad, Iraq

Received: 7th June, 2021; Revised: 20th July, 2021; Accepted: 1st August, 2021; Available Online: 25th September, 2021

ABSTRACT

A new set of metal complexes by the general formula $[M(C)_2(H_2O)_2]Cl_2$ has been prepared through the interaction of the new Ligand [N1, N4-bis(4-chlorophenyl)succinamide] (C) derived from succinyl chloride with 4-Chloroaniline with the transition metal ions Mn(II), Co(II), Ni(II), Hg(II), Cu(II) and Cd(II). Compounds diagnosed by TGA, ¹H, ¹³CNMR and Mass spectra (for (C)), Fourier-transform infrared and Electronic spectrum, Magnetic measurement, molar conduct, (%M, %C, %H, %N). These measurements indicate that (C) is associated with the metal ion in a bi-dentate fashion by nitrogen atoms (the amide group) and the octahedral composition of these complexes is suggested. The anti-bacterial action of the compounds towards three types of bacteria *Pseudomonas* (+), *Staphylococcus aureus* (+), and *Escherichia Coli* (-) were studied.

Keywords: 4-Chloroaniline, Biological activity, Succinyl chloride

International Journal of Drug Delivery Technology (2021); DOI: 10.25258/ijddt.11.3.13

How to cite this article: Abdulrahman WA, Othman IA, Waheed EJ. Metal Complexes of Ligand Derived from Amine Compound: Formation, Spectral Characterization, and Biological Evaluation. International Journal of Drug Delivery Technology. 2021;11(3):728-734.

Source of support: Nil.

Conflict of interest: None

INTRODUCTION

Aniline is one of the most organic compounds (toxic). Aniline is involved in synthesizing many organic compounds via azo dyes, corrosion inhibitors, pesticides, antioxidants, rubber, antiseptics, pharmaceuticals, and fuel additives, due to the wastewater structure for pharmaceutical production dyestuffs and its high toxicity due to its aniline content harm aquatic ecosystems.^{1,2} Aniline derivatives contribute to the manufacture of paints, pharmaceuticals, rubber, dyes, herbicides, pigments, and precursors to polyurethane. Although aniline compounds produced in some pharmaceutical factories are organic, they are very complex in composition, causing high resistance to biological degradation.³ 4-Chloroaniline is aromatic amine-containing chlorine substituted for the benzene ring and is used as a medium during the degradation (microbial) of phenyl carbamate with phenylurea. Polymerizing it with guaiacol in an aqueous solution containing oxido reductases creates different oligomers.^{4,5} It can be used in these industries (azo dyes, cosmetics, agricultural chemicals, pharmaceutical products, and pigments) as an intermediary. Hemoglobin and liver and kidney proteins covalently bind with metabolites reactions to 4-Chloroaniline. Due to continuous exposure to it, several damages to human health are cyanosis, methemoglobinemia, effects in blood, kidneys, liver, spleen, changes in hematological parameters, and haemosiderosis in

the spleen.⁶⁻⁸ The current study aims to define the structure and geometry of (C) and its complexes to ions Mn(ii), Co(ii), Ni(ii), Hg(ii), Cu(ii), and Cd(ii).

EXPERIMENTAL SECTION

Materials and Methods

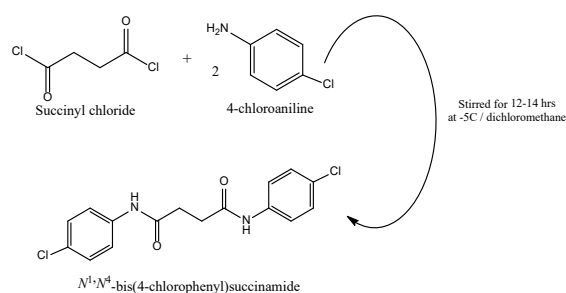
From commercial sources, we obtained all chemical and analytical reagents and were used without further purification. From (the United States of America, Sigma - Aldrich, Merck, and India), various chemicals, metal salts, and solvents used in this research were purchased. Infrared spectroscopy was measured using the device (Shimadzu FTIR affinity-1s) and KBr disc within the range (400–4000) cm^{-1} . Using an electrothermal melting point device (SMP10 Stuart), the melting point of the compounds prepared in an open tube was determined. Using (Shimadzu UV-1800) visible, ultraviolet spectrophotometer with a concentration of 3^{-10} M samples in dimethylsulfoxide (DMSO) solvent at room temperature and a quartz cell length of 1.0 cm, the electron spectra of the prepared compounds were measured. Using the device (Bruker 300 MHz NMR spectrometer), the chemical displacements were recorded in (NMR spectra ¹H and ¹³C) in DMSO-d₆ with trimethylsilyl (TMS). Using a device (Shimadzu (AA 680)), %M in complexes is determined. Using a device (Philips pw-Digital conductivity meter), the molar conductivity of

the prepared compounds was measured with a concentration of 10^{-3} M in DMSO and at room temperature. Using a device (magnetic sensitivity balance (Sherwood Scientific)), (μeff BM) of complexes were measured at room temperature. Using a device (Euro EA 300), (%C, %H, %N) was determined for the prepared compounds. An STA PT-1000 Linseis at the temperature range of 0–1000 °C and used argon gas, thermal gravity analysis (TGA) was performed.

The Organic Compound

Synthesis of Ligand (C)⁹

A solution of (0.999 g, 6.45 mmol) of Succinyl chloride in acetone (10 mL) was slowly added to a solution of 4-Chloroaniline (1.645 g, 12.9 mmol) in dichloromethane 10 mL over 1-hour. The mixture was stirred for 12 hours at -5 °C and then for 2 hours at laboratory temperature. The precipitate



Scheme 1: Preparation course of the (C)

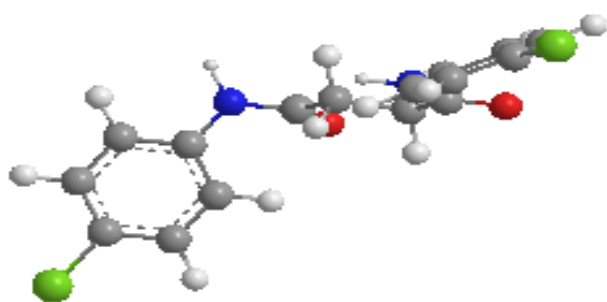


Figure 1: 3D-Structure of the (C)

formed was filtered and then washed with solvents (water and diethyl ether) and then recrystallized in ethanol and left to dry at laboratory temperature. m.p. 160–163 °C (yield 88%) (Scheme 1 and Figure 1).

In-Organic Compounds

Synthesis of $[M(C)_2(H_2O)_2]Cl_2$: To ligand (C) solution (0.66 gm, 2 mmol) in (10ml) EtOH, the metal chloride solution ($MnCl_2 \cdot 4H_2O$, $CoCl_2 \cdot 6H_2O$, $NiCl_2 \cdot 6H_2O$, $CuCl_2 \cdot 6H_2O$, $HgCl_2 \cdot H_2O$ and $CdCl_2 \cdot H_2O$) (0.24–0.17 gm, 1 mmol) in (10ml) EtOH was added. Under reflux, the reaction mixture was heated for 4 hours. The precipitate formed was filtered and then washed with solvents (H_2O and diethyl ether) and then recrystallized in ethanol and left to dry at laboratory temperature (Figure 2)

RESULTS AND DISCUSSION

Thermal stability and the nature of the colored solid are the essential characteristics of the prepared metal complexes. In solvents DMSO and dimethylformamide (DMF), soluble. The theoretical and practical data of (AA) measurements for all prepared complexes were approximated (Table 1).

Mass Spectral

The mass spectral data fragmentation of (C) [N_1, N_4 -bis(4-chlorophenyl)succinamide], Figure 3 showed ($M+$)

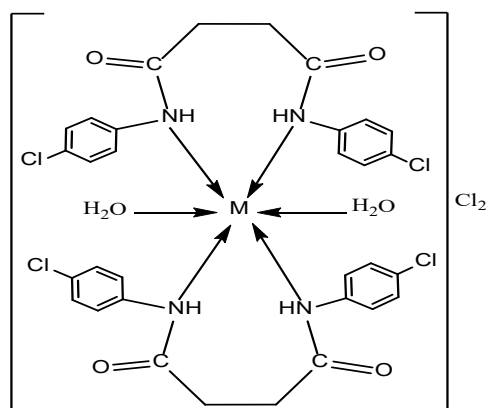


Figure 2: Suggested structure for (C) complexes

Table 1: Different physical properties of the prepared compounds

Compound	Empirical Formula (Formula wt.)	m.p. (°C)	Color	Metal% Calculated (Actual)	Conducts $\text{Ohm}^{-1}\text{cm}^2\text{mol}^{-1}$ In solvent (DMSO)
Ligand (C)	$C_{16}H_{14}Cl_2N_2O_2$ 337.20	160–163	Yellow	-----	1.68
Mn-C	$C_{32}H_{32}Cl_6MnN_4O_6$ 836.27	188–190	Off-White	6.57 (6.56)	74.3
Co-C	$C_{32}H_{32}Cl_6CoN_4O_6$ 840.26	197–200	Green	7.01 (7.03)	75.5
Ni-C	$C_{32}H_{32}Cl_6NiN_4O_6$ 840.02	117–120	Green	6.99 (7.01)	72.1
Cu-C	$C_{32}H_{32}Cl_6CuN_4O_6$ 844.88	168–170	Brown	7.52 (7.51)	70.4
Cd-C	$C_{32}H_{32}Cl_6CdN_4O_6$ 893.74	214–216	Yellow	12.58 (12.56)	81
Hg-C	$C_{32}H_{32}Cl_6HgN_4O_6$ 981.92	177–180	Yellow	20.43 (20.44)	69

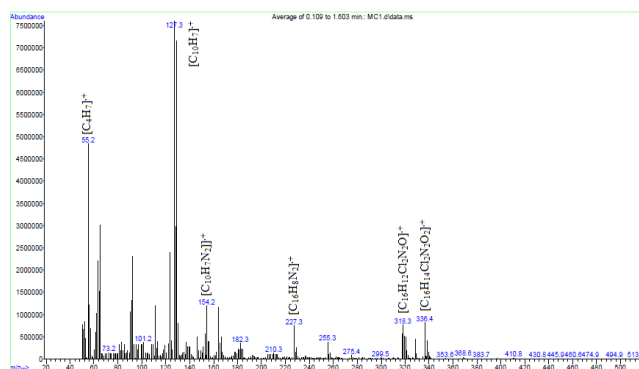


Figure 3: EI mass spectrum of (C).

Table 2: The fragmentation pattern of (C)

Fragment	Mass/charge (m/z)	Relative abundance
$[C_{16}H_{14}Cl_2N_2O_2]^+$	336	12%
$[C_{16}H_{12}Cl_2N_2O]^+$	318	12%
$[C_{16}H_8N_2]^+$	227	9.3%
$[C_{10}H_7N_2]^+$	154	22.7%
$[C_{10}H_7]^+$	127	100%
$[C_4H_7]^+$	55	64%

at ($m/z=336$) Due to (the original molecular weight of C) (337), $[C_{16}H_{14}Cl_2N_2O_2]$. Additional peaks are displayed in Table 2.^{10,11}

Nuclear Magnetic Resonance (NMR) Spectra

¹H-NMR Spectra of (C)

In order to confirm the structure of the ligand (C), ¹H-NMR of the synthesized ligand was recorded. Figure 4 displays the ¹H-NMR of (C), the peak at (δ 10.25–10.29 ppm) corresponds to the proton of NH group. The peaks at (δ 7.23– δ 7.82 ppm) correspond to all the aromatic protons of the ligand. The peak at (δ 2.71–2.78 ppm) corresponds to four aliphatic protons of the succinyl group. Finally, the peaks at (δ 2.47–2.58 ppm) correspond to residual protons in DMSO-d₆ and moisture protons in DMSO-d₆.^{12,13} The results are summarized in Table 3.

¹³C-NMR Spectra of (C)

The ¹³C-NMR spectrum for ligand (C) portrayed is shown in Figure 5. The spectrum exhibits signals at chemical shift ($\delta=177.17$ ppm), which assign to (C_{1,1'}). The chemical shifts at ($\delta=138.76$, 135.99, 129.28–129.82 and 120.91 ppm) attributed to the aromatic ring (C_{2,2'}), (C_{3,3'}), (C_{4,4'}) and (C_{5,5'}) respectively. Chemical shift at ($\delta=39.10$ –40.78 ppm) related to DMSO-d₆. Finally chemical shift at ($\delta=31.52$ –31.63 ppm) attributed to (C_{6,6'}).^{14,15}

Fourier Transform Infrared Spectroscopy (FTIR) Spectra

Ligand (C)

The band at 3299 cm⁻¹ the spectrum of (C) determined to the ν (NH), while another absorption band showed at (1652) cm⁻¹ could be interpreted as ν (C=O amide), in addition to

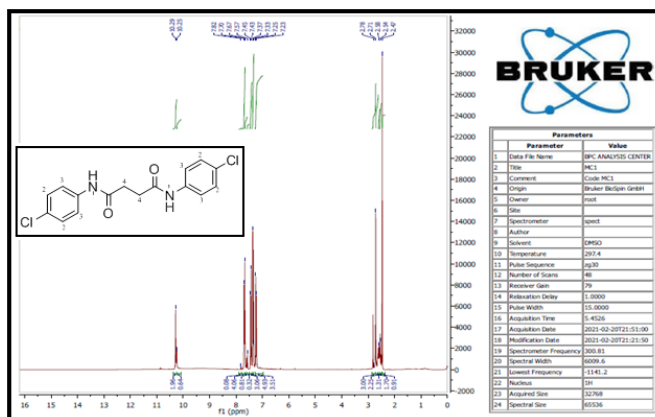


Figure 4: ¹H-NMR spectra of (C)

Table 3: Chemical shifts in (¹H-NMR) spectra of (C)

Compound	Functional groups	δ (ppm)
Ligand (C)	proton (N-H) group	10.25–10.29 (2H),d
	Aromatic protons C(2,2'),(3,3')	7.23–7.82 (8H),m
	succinyl group protons C(4,4')	2.71–2.78 (4H),d
	DMSO-d ₆	2.47–2.58

m = multiplet, d = doublet

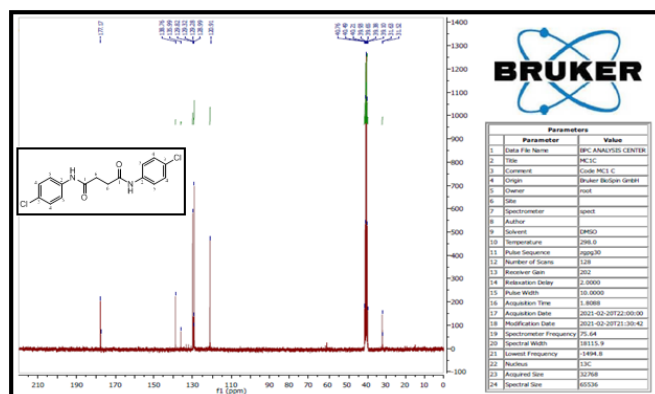


Figure 5: ¹³C-NMR spectra of (C)

Table 4: Chemical shifts in (¹³C-NMR) spectra of (C)

Compound	Functional groups	δ (ppm)
Ligand (C)	C _{1,1'} for (CO-NH) amide group	177.71
	C _{2,2'} for aromatic ring	138.78
	C _{3,3'} for aromatic ring	135.99
	C _{4,4'} for aromatic ring	129.28-129.32
	C _{5,5'} for aromatic ring	120.91
	C _{6,6'} for (CH ₂) Succinyl group	31.52-31.63
DMSO		39.10-40.78

absorption bands at (2921) due to ν (C-H aliphatic), (3053) cm⁻¹ due to ν (C-H aromatic) and (2835) cm⁻¹ which determined to ν (C-Cl), Figure 6.¹⁶

Complexes of Ligand (C)

These spectra showed a marked various between bands belonging to the stretching vibration of ν (NH, amide group) in the range between (3427–3402) cm⁻¹ shifted to higher

frequencies by 128–103 cm^{-1} proposing the probability of the coordination of (P) by the nitrogen atom at the amide group.^{17,18} The $\nu(\text{C}=\text{O}$, amide) in ligand was not correlated with the central ion and confirmed by no changes in frequencies of this group set at (1654–1649) cm^{-1} in the complexes spectrum of the ligand complexes.^{19,20} New bands $\nu(\text{M}-\text{O}$, water group) and $\nu(\text{M}-\text{N}$, amide group) appeared in the range of (823–819) cm^{-1} and (487–495) cm^{-1} , respectively, indicating the formation of the metal complexes.^{21,22} In Table 5, FTIR data is displayed. In Figure 7, the spectra of the (C) and its complexes were presented.

Electronic Spectra

Ligand (C)

The electronic spectrum of (C) in DMSO solution is including in Figure 8. The spectrum display absorption peaks (two) at (254 nm = 39370 cm^{-1} ; $\epsilon_{\text{max}} = 3720 \text{ molar}^{-1} \text{ cm}^{-1}$ and (292 nm = 34246 cm^{-1} ; $\epsilon_{\text{max}} = 3853 \text{ molar}^{-1} \text{ cm}^{-1}$ which assigned to ($n \rightarrow \pi^*$) and ($\pi \rightarrow \pi^*$) respectively.²³ In Table 6 data are recorded.

Complexes of Ligand (C)

The electronic spectrum of the Mn (ii) - complex display peaks in the (d-d) region at 887 nm, which is due to ${}^6\text{A}_{1g} \rightarrow {}^4\text{T}_{2g(\text{G})}$ transition and 910 nm assigned to ${}^6\text{A}_{1g} \rightarrow {}^4\text{T}_{1g(\text{G})}$. Another peak in the 275 nm and 314 nm which assigned to intra ligand, these peaks indicating octahedral geometry about Mn ion.²⁴

The Co (ii) - complex show peak at 272 nm and 310 nm attributed to intra ligand. Another peak in the (d-d) region 600 is due to ${}^4\text{T}_{1g(\text{F})} \rightarrow {}^4\text{A}_{2g(\text{P})}$ transition and 680 due to ${}^4\text{T}_{1g(\text{F})} \rightarrow {}^4\text{T}_{2g(\text{F})}$. These electronic transitions revealed by the

cobalt complex refer to the octahedral geometry of the aforementioned complex.²⁵

The electronic spectrum of the Ni^{II} - complex display in the (d-d) region (peaks) at 686 nm assigned to ${}^3\text{A}_{2g} \rightarrow {}^3\text{T}_{1g(\text{P})}$ transition and 774 nm due to ${}^3\text{A}_{2g} \rightarrow {}^3\text{T}_{2g(\text{F})}$. Other peaks at 272 nm and 312 nm due to intra ligand indicate octahedral geometry about Ni ion²⁶ (Figure 9).

The electronic spectrum of the Cu (ii)- complex display in the (d-d) region (peak) at 944 nm attributed to ${}^2\text{E}_g \rightarrow {}^2\text{T}_{2g}$. Another peak at 264 nm and 310 nm due to intra ligand, these all confirming distorted octahedral geometry about Cu ion.²⁷

The electronic spectra of the Cd-complexes exhibited peaks at (267, 310) nm, which were due to (intra-ligand) and another peak at 399 nm due to (CT) and the Hg-complexes exhibited peaks at (278, 310) nm, which were due to (intra-ligand) and another peak at 410 nm due to CT. These are all indicating octahedral geometry about Cd and Hg ions.²⁸ In Table 6, UV data of compounds was displayed.

Magnetic Moments and Conductivity Measurements

In Table 5, the $\mu(\mu_{\text{eff}})$ values of Mn(ii), Co(ii), Ni(ii), and Cu(ii) complexes are display. These complexes exhibit μ_{eff} (5.494, 4.370, 3.491 and 2.134) B.M respectively, these normal values are consistent with high spin octahedral complexes.²⁹ The electrolytes nature (1:2); $\text{M}^{+2} = \text{Mn}(\text{ii}), \text{Co}(\text{ii}), \text{Ni}(\text{ii}),$ and Cu(ii), Hg(ii) and Cd(ii) complexes of all metal complexes was confirmed by molecular conductivity measurements,³⁰ (Table 1).

Table 5: FT-IR data of (C) (cm^{-1}) and their complexes.

Comp.	$\nu(\text{C}-\text{H})$ Arom.	$\nu(\text{C}-\text{H})$ Aliph.	$\nu(\text{N}-\text{H})$	$\nu(\text{C}=\text{O})$ amide	$\nu(\text{C}-\text{Cl})$	$\nu(\text{M}-\text{N})$	$\delta(\text{M}-\text{O})$ of water
Ligand (C)	3053	2921	3299	1652	721	-	-
Mn-C	3033	2925	3421	1650	717	823	487
Co-C	3051	2904	3402	1650	717	821	491
Ni-C	3053	2920	3423	1649	717	821	491
Cu-C	3035	2991	3413	1654	717	819	489
Cd-C	3014	2929	3421	1652	717	823	487
Hg-C	3037	2927	3427	1652	713	821	495

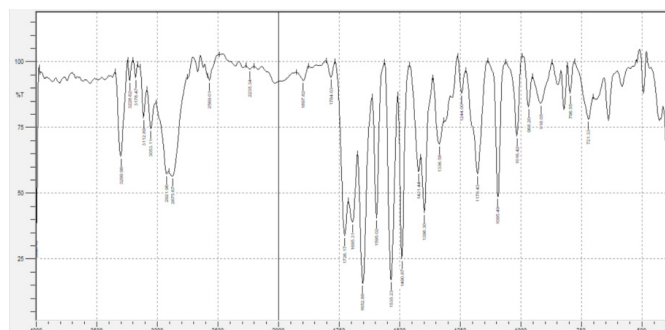


Figure 7A: FTIR spectrum of [C] complex.

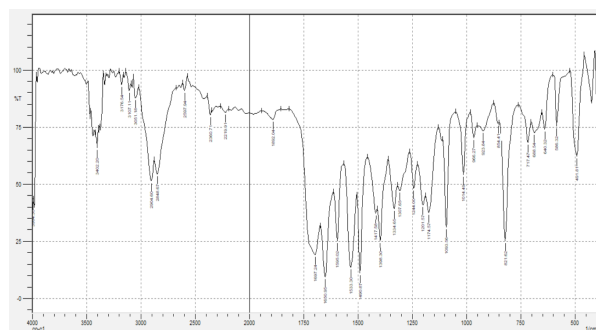


Figure 7B: FTIR spectrum of [Co-C] complex.

Thermal Analysis

The ligand (C) was prepared and subjected to thermal analysis using a STAPT-1000 Linseis company Germany. In an atmosphere of argon gas, this measurement was done

Table 6: Electronic transfers in the spectra of the prepared compounds

Com.	λ_{max} (nm)	ν (cm^{-1})	ϵ_{max} ($mole^{-1} \cdot cm^{-1}$)	Transition	Shape geometry
Ligand (C)	254	39370	3720	$n \rightarrow \pi^*$	-
	292	34246	3853	$\pi \rightarrow \pi^*$	
Mn-C	215	36363	3768	Intra-ligand	Octahedral
	314	31847	3653	Intra-ligand	
	887	11273	15.8	${}^6A_{1g} \rightarrow {}^4T_{2g}(G)$	
	910	10959	16.2	${}^6A_{1g} \rightarrow {}^4T_{1g}(G)$	
Co-C	272	36764	7048	Intra-ligand	Octahedral
	310	32258	6920	Intra-ligand	
	600	16667	212.9	${}^4T_{1g}(f) \rightarrow {}^4A_{2g}$	
	680	14705	428.9	${}^4T_{1g}(f) \rightarrow {}^4T_{2g}(f)$	
Ni-C	272	36764	7048	Intra-ligand	Octahedral
	312	32051	3597	Intra-ligand	
	686	14577	17.2	${}^3A_{2g} \rightarrow {}^3T_{1g}(f)$	
	774	12919	16.8	${}^3A_{2g} \rightarrow {}^3T_{2g}(f)$	
Cu-C	264	37878	7222	Intra-ligand	Octahedral
	310	32258	6920	Intra-ligand	
	944	10593	264.1	$2E_g \rightarrow 2T_{2g}$	
Cd-C	267	36231	7390	Intra-ligand	Octahedral
	310	32258	7429	Intra-ligand	
	399	25062	132.9	C.T	
Hg-C	278	35971	7369	Intra-ligand	Octahedral
	310	32258	7001	Intra-ligand	
	410	24390	628.5	C.T	

within the temperature range (0–1000)°C and heating rate 10°C/min.^{31,32} Where it was recorded, all results are derived from the TG curves for the ligand (C) examined (Table 7 and Figure 10).

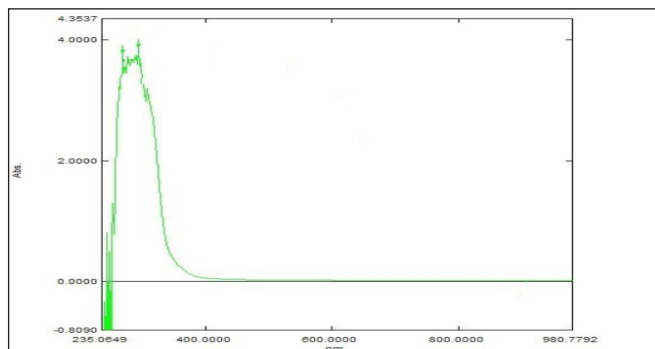


Figure 8: Electronic spectrum of the C.

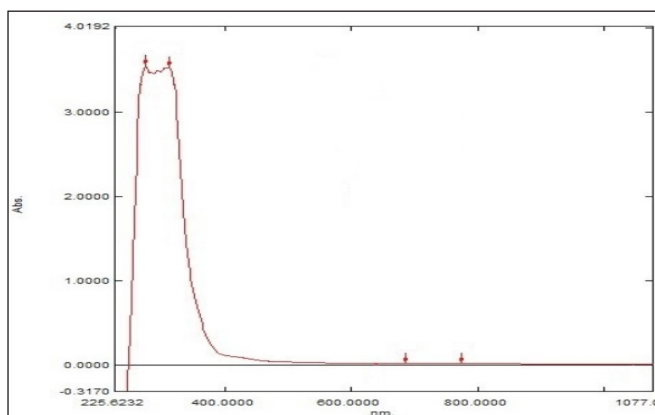


Figure 9: Electronic spectrum of [Ni-C] complex density.

Table 7: Temperature values for analysis along with corresponding weight loss values

Com.	Stage	TGA		Found (calculate)		
		Thermo Gravimetry range (°C)	loss of Mass (mg)	Total mass lose(mg)	Fragmentation	
Ligand (C)	1	160–250	2.056 (2.046)	5.464	- C ₂ H ₆ , 1/2Cl ₂ , N ₂ O ₂	
	2	251–40	2.742(2.741)	(5.441)	-11C + 1/2 Cl	
	3	341–1000	0.665(0.654)		-C ₃ H ₄	

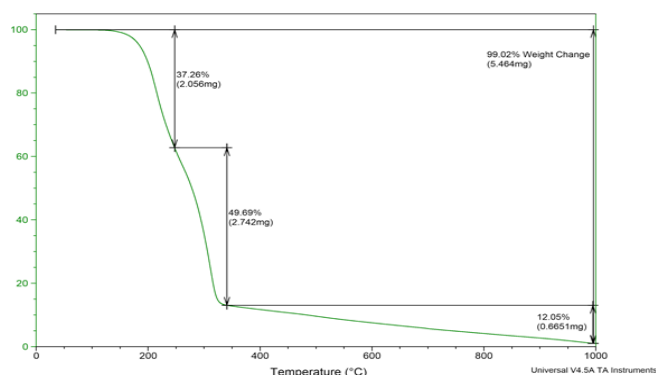


Figure 10: Thermal study of (C)

Table 9: Results obtained from the biological activity of the prepared compounds.

No.	Compound	<i>Escherichia coli</i> (G -)	<i>Pseudomonas</i> (G -)	<i>Staphylococcus aureus</i> (G +)
	Control	-	-	-
1	Ligand C	4	8	-
2	[Mn(C) ₂ (H ₂ O) ₂]Cl ₂	14	-	-
3	[Co(C) ₂ (H ₂ O) ₂]Cl ₂	9	10	-
4	[Ni(C) ₂ (H ₂ O) ₂]Cl ₂	9	-	9
5	[Cu(C) ₂ (H ₂ O) ₂]Cl ₂	14	4	5
6	[Cd(C) ₂ (H ₂ O) ₂]Cl ₂	19	12	-
7	[Hg(C) ₂ (H ₂ O) ₂]Cl ₂	4	29	-

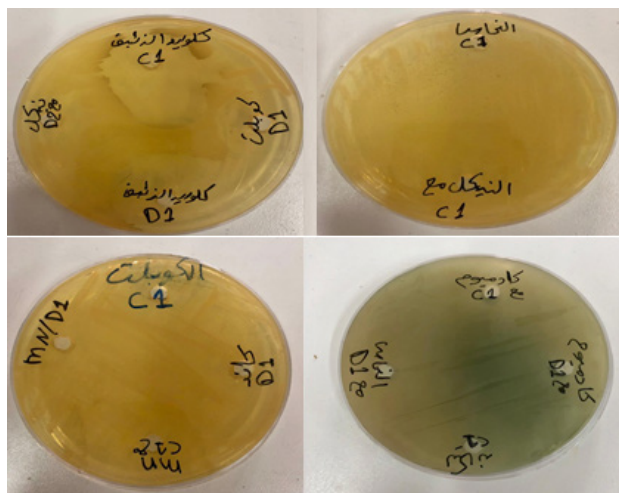


Figure 13: Figures of the biological activity of the prepared compounds

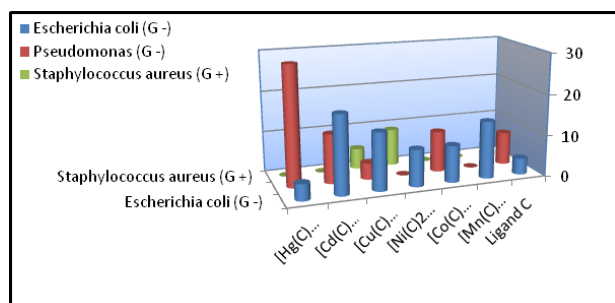


Figure 14: Graph of the results of the bioactivity of the prepared compounds

Anti-bacterial Activity Studies

Pseudomonas (+), *Staphylococcus aureus* (+), and *Escherichia Coli* (–) were used as test micro-organisms. The medium surface was inoculated and covered to perform the assay on test organisms. Before applying disks, allow the agar surface to dry for 3 to 5 minutes. The tablets were dipped in a chemical beaker using sterile forceps and placed in the medium previously. To grow the bacteria, plates were incubated at 37°C for 48 hours. The complexes show different activity in limiting bacterial proliferation compared to ligand (C) in concentrations prepared.³³⁻³⁴ The results obtained are recorded (Table 8, Figure 11 and 12)

CONCLUSION

This search showed the prepared and identification of (C) and its Mn (ii), Co (ii), Ni (ii), Cu (ii), Hg (ii), and Cd (ii) compounds. The octahedral geometry of the prepared complexes was suggested depending on the results (TGA, ¹HNMR, Mass spectra, and ¹³CNMR of (C) only), magnetic measurement, and molar conductivity of the compounds. The (C) acts as bidentate and coordinates by the N atoms in (NH-C=O) group. The thermal decomposition steps of the different parts of the prepared ligand (C) were determined by studying TGA. The (C) and its complexes were examined for their anti-bacterial activities against three types of bacteria.

REFERENCES

1. Leela S, Rani TD, and Subashini A. Studies on growth and characterization of nonlinear optical material 4-chloro-40methoxy benzylideneaniline: A Schiff base organic material. *Arabian Journal of Chemistry*, 2017;10:S3974-S3981.
2. Sobola AO, Watkins GM and Brecht BV. Synthesis, Characterization and Antimicrobial Activity of Copper(II) Complexes of some Ortho-substituted Aniline Schiff Bases; Crystal Structure of Bis(2-methoxy-6-imino)methylphenol Copper(II) Complex. *S. Afr. J. Chem.*, 2014;67:45-51.
3. Jaiswal N, Kushwah AK and Pratap A. Synthesis, spectroscopic characterization and computational studies of Schiff base complexes of tin(IV) chloride. *Main Group Met. Chem.*, 2019;42:28-36.
4. Patel V, Trivedi P and Gohel H. Synthesis and Characterization of Schiff Base of p - chloro aniline and their Metal Complexes and their evaluation for Antibacterial Activity. *IJAPBC*, 2014;3(4):156-169.
5. Sridhar G, Bilal M, and Easwaramoorthy D. Synthesis, Characterization and Antimicrobial Activities of Copper, Nickel, Cobalt, Chromium Complexes Derived from (Z)-4-Fluoro-N-(2,7-dimethylhept-6-enylidene) benzenamine. *J. Braz. Chem. Soc.* 2017;28(5):756-767.
6. Bahule B, Kalaskar SB, and Yadav RP. Synthesis, Characterisation and Biological Study of Nickel Complexes Derived from Schiff Bases of p-nitro Aniline and m-nitro Aniline with Aromatic Aldehydes. *Int. J. Adv. Res.* 2017;2(7):5708-5715.
7. Geete A, Shrivastava BD, and Mishra A. XRD Study of Cobalt [Co(ii)] Complexes Synthesized with Ligands of Aniline/Toluidine Dithiocarbamate. *Rasayan J. Chem.*, 2020;13(3):1878-1884.
8. Abbas SH, Ali DM, and Abbas HH. Spectral and cyclic voltammetry studies of chloro-salicyliden aniline and some of its complexes with Co(II) and Mn(II). *Journal of Physics: Conference Series*, 2020;1660:1-11.
9. Asma M, Badshah A, and Ali S. Synthesis and Anti-bacterial Application of Copper (II) Salicyldehyde Schiff Base Complex. *Austin J Anal Pharm Chem.* 2016;3(4):1077-1145.
10. Durrani A, Kayande DDM and Pardeshi RK. Binary complexes of N-[2-hydroxy-1-naphthalidene]-2-chloroaniline with transition elements. *J. Chem. Pharm. Res.*, 2015;7(12):813-815.
11. Al-Khodir AIF, Abumelha MAH. New Platinum(IV) and Palladium(II) Transition Metal Complexes of s-Triazine Derivative: Synthesis, Spectral, and Anticancer Agents Studies. *BioMed Research International.* 2019;4:1-14.
12. K. RajendraJain and A. P. Mishra. Microwave synthesis, spectral, thermal, and antimicrobial activities of some transition metal complexes involving 5-bromosalicylaldehyde moiety. *Current Chemistry Letters* 1. 2012, 163-174.
13. Chellali EJ, Keely C, and Bell G. Cobalt and zinc halide complexes of 4-chloro and 4-methylaniline: Syntheses, structures and magnetic behavior. *Polyhedron*, 2019;168:1-10.
14. Kong S, Guo C, and Yang W. 2,6-Dibenzhydryl-N-(2-phenyl imino) naphthylidene)-4-chloroaniline nickel dihalides: Synthesis, characterization and ethylene polymerization for polyethylenes with high molecular weights. *Journal of Organometallic Chemistry.* 2013;725:37-45.
15. Enass JW. "Synthesis, Spectral and Thermal Characterization of Ni(II), Cu (II) and Zn(II) Complexes with New Ligand Towards Potential Biological Application." *Biochemical and Cellular Archives*, 20.1. 2020;2483-2494.

16. Alias FM, Seewan NA. Synthesis, Spectral Study, Theoretical Treatment and Biological Activity of Some Transition Metal Complexes with 2-Amino Acetic Acid-6-Chloro Benzothiazole. DJPS. 2013;9(4):93-103.
17. Molano FM, Lorett PV, and Mauricio F. Crystal structures of organoplatinum complexes containing alkylleugenoxyacetate and p-chloroaniline. Acta Cryst. 2016;E72:912-917.
18. M. Molani, L. Vanezai . Crystal structure, spectroscopic characterization and Hirshfeld surface analysis of aquadichlorido {N-[(pyridin-2-yl)methylidene]aniline}copper(II) Monohydrate. Acta Cryst. 2020;76(2):48-154.
19. Sarhan, Basima M., Nada J. Kadhim, and Enas J. Wheed. "Stability constant of some Metal Ion Complexes of (6-(2-Amino-2-(4-hydroxy phenyl)-acetamido)-3, 3-di methyl-7oxo-4-thia-1-aza-bicyclo [3, 2, 0] heptanes-2carboxylic acid (Amoxicillin)." *Ibn AL-Haitham Journal For Pure and Applied Science* 26.3 (2017): 245-253.
20. Subashini K, Priyadharsani P, and Thamaraiselvi K. Synthesis, growth and characterization of dichlorobis(4-chloroaniline-κN) zinc semiorganic crystal. Journal of Materials Science: Materials in Electronics. 2018;29:4147-4154.
21. M. Rani, S. Sathiya and M.Vimala. Synthesis, Characterization and Biological Activity of Transition Metal Complexes Supported. IJEAT. 2015;4(7):2249 - 8958.
22. Enass WJ, and Awf ARA. "Synthesis, Characterization, Thermal Study, Biological Activity and Corrosion Inhibition of New Ligand Derived from Butanedioyl Dichloride and Some Selective Transition Metal Complexes." Journal of Global Pharma Technology 11.2 (2019): 379-391.
23. Hoseyni SJ, Manoochehri M, and Asli MD. Synthesis of Cobalt nanoparticles by Complex Demolition Method Using the Reaction between Organic Ligand Schiff base and Cobalt Chloride by Ultrasonication. Bulletin de la Société Royale des Sciences de Liège. 2017;86:182-188.
24. Sarhan, Basima M., Sajid M. Lateef, and Enass J. Waheed. "Synthesis and Characterization of Some Metal Complexes of [N-(1, 5-dimethyl-3-oxo-2-phenyl-2, 3-dihydro-1H-pyrazol-4-ylcarbamothioyl) acetamide]." *Ibn AL-Haitham Journal For Pure and Applied Science* 2017;28(2):102-115.
25. L. Yamilka Salina-Aguilera, C. Armando Ferrer- Serrano and F. Nápoles-Escutary I. Copper (II) and zinc (II) with 2-(4-Chloroaniline)-1,2-Diphenyl-1-Ethano nethiosemicarbazone in Solution: Possible Competition for Ligand. Coordination Sites. Revista Cubana de Química, págs. 2014;2(5):94-103.
26. L. Nimmy John, K. Lija Joy and M. Saravana Kumar. Quantitative structure and activity relationship on the biological, nonlinear and the spectroscopic properties of the Schiff base material: 4-chloro-4'-bromobenzylidene aniline. Molecular Simulation, 2017;1-15.
27. Enass, J. Waheed, et al., "Synthesis And Characterization of New Manganese(II), Cobalt(II), Cadmium(II) and Mercury (II) Complexes with ligand [N-(3-acetylphenylcarbamothioyl)-2-chloroacetamide] and their Antibacterial Studies", Conf. Series: Journal of Physics 1234 (2019):1-11.
28. Dunstan PO and Khan AM. Thermochemical Parameters of 3-Chloroaniline Complexes of Certain Bivalent Transition Metal Bromides. Open Journal of Physical Chemistry. 2013;3: 163-169.
29. Park S, Lee KJ and Lee H. Zinc (II), palladium (II) and cadmium (II) complexes containing 4-methoxy-N-(pyridin-2-ylmethylene) aniline derivatives: Synthesis, characterization and methyl methacrylate polymerization. Appl Organometal Chem. 2019, 4797:1-15.
30. Association Equilibria of Co(II) and Cu(II) Complexes of Salicylidine p-chloroaniline in Different Solvents. Sci. 2013;24(2): 55-69.
31. R. Sharma, B. Reddi and S. Bhattacharya. Synthesis, crystal growth, structural and physico-chemical studies of novel binary organic complex: 4-chloroaniline-3-hydroxy-4-methoxy benzaldehyde. Journal of Solid State Chemistry. 2012;190:226-232.
32. G. Subashini Bhagavannarayana and K. Ramamurthi. Synthesis, growth, crystalline perfection of 4-bromo-4'-dimethylamino benzylideneaniline (BDMABA) and photons absorption of BDMABA crystal. Molecular and Biomolecular Spectroscopy 2013;104:403-408.
33. Tukur A and Isah AY. Physical Science & Biophysics Journal Committed to Create Value for Researchers Synthesis, Characterization and Antimicrobial Studies of 2-[(E)-[(4-Chlorophenyl)Imino]Methyl]Phenol Schiff Base Ligand and its Cu(II) Complex Synthesis, Characterization and Antimicrobial Studies of 2-[(E)- [(4-Chlorophenyl)Imino]Methyl]Phenol Schiff Base Ligand and its Cu(II) Complex. Phys. sci. 2020;4(2): 159:1-6.
34. Subashini A, Leel S and Ramamurthi K. Synthesis, growth and characterization of 4-bromo-4'-nitrobenzylidene aniline (BNBA): a novel nonlinear optical material with a (3+1)-dimensional incommensurately modulated structure. Cryst Eng Comm, 2013;15:2474-2481.